



ELSEVIER

Desalination 188 (2006) 251–262

DESALINATION

www.elsevier.com/locate/desal

Direct contact membrane distillation mechanism for high concentration NaCl solutions

Yanbin Yun^{a,b*}, Runyu Ma^b, Wenzhen Zhang^c, A.G. Fane^c, Jiding Li^a

^aDepartment of Chemical Engineering, Tsinghua University, Beijing, 100084, China

Tel. +86 (10) 6278-2432; Fax +86 (10) 6277-0304; email: yuanyb@mail.tsinghua.edu.cn

^bSchool of Chemical Engineering, Beijing University of Chemical Technology, Beijing, 100029, China

^cSchool of Chemical Engineering and Industrial Chemistry, The University of New South Wales,
Sydney, NSW, 2052, Australia

Received 1 November 2004; accepted 29 April 2005

Abstract

Using high concentration NaCl aqueous solutions, direct contact membrane distillation (DCMD) experiments are implemented in this work where water fluxes are measured at different feed/permeation temperatures, feed concentrations and flow rates. The results under the experimental conditions show that (1) water fluxes decrease as concentrations of NaCl solutions increase; (2) when concentrations of NaCl solutions are above 25%, water fluxes decrease sharply; (3) when concentrations of NaCl solutions are up to saturation, water fluxes gradually approach steady levels. Variations of membrane-fouling resistance are found to result in the above observations. Analysis also shows that concentrations of NaCl solutions, operation temperatures and flow rates can affect the speed of membrane fouling. Among them, the concentration is the most important factor. In this work, a new model is also proposed which takes membrane resistance, concentration polarization resistance and membrane fouling resistance all into consideration. Model predictions show good agreement with the experimental results.

Keywords: Membrane distillation; Micro-porous PVDF membrane; Mass and heat transfer

1. Introduction

With increasing demands for fresh water around the world, seawater desalination techno-

logy has been developing quickly in the past decades. Because of its low energy consumption, accessible running conditions and simple maintenance, membrane distillation (MD) or reverse osmosis (RO) has become one of the cheapest technologies for seawater desalination. The

*Corresponding author.

Presented at the International Conference on Integrated Concepts on Water Recycling, Wollongong, NSW Australia, 14–17 February 2005.

coefficient of water recovery is often addressed by the energy consumption per ton fresh water. If the coefficient is high, the energy consumption is low. Nowadays, the typical coefficient of water recovery is 30~40% for RO seawater desalination technology. Therefore, improving the coefficient of water recovery is a key issue for studying the RO technology. However, it is also known that if the coefficient of water recovery is improved, osmotic pressure of seawater will rise. As a result, the scale will be formed on the membrane surface and the permeate flux will fall. Currently, there are some methods to improve the coefficient of water recovery using RO, e.g., (1) improving operating pressure; (2) improving operation temperature; (3) adding pre-treatment equipment. These methods can improve operating charges significantly.

Membrane distillation (MD) is an evaporation process of feed volatile components through porous hydrophobic membrane. For DCMD configuration, the surfaces of the membrane are in direct contact with two liquid phases, hot liquid and cold liquid, kept at different temperatures. Inside the pores, only a gaseous phase is present, through which vapor is transported as long as a partial pressure difference is maintained. The evaporation takes place at the feed-membrane interface. The vapor flows through the membrane pores and condenses at the permeate-membrane interface. This process is the same as conventional distillation processes, i.e., evaporation-transportation-condensation. The driving forces for the separation are represented by the partial pressure gradient for the evaporating species, maintained by a suitable temperature difference between the evaporation and condensation surfaces.

The main advantages of membrane distillation over conventional separation processes are [1]:

- (1) Complete separation (in theory) of ions, macromolecules, colloids, cells etc.,
- (2) Lower operating temperatures and pressures,
- (3) Lower membrane mechanical intensity demand.

The direct contact membrane distillation (DCMD) configuration, which is simple to operate and requires the least equipment, is best suited for applications in which the major permeate component is water, such as desalination or the concentrations of aqueous solutions [2–4]. In the literature, the heat and mass transfer mechanisms were studied widely for low concentration solutions [5]. However, membrane distillation mechanism for high concentration solution has not been reported in the literature due to its complexity. The complexity may be caused by changes of many operating parameters, such as decrease of the feed vapor pressure, increase of the feed viscosity and permeate pressure, which decreases evaporation efficiency.

In this work, direct contact membrane distillation mechanism for high concentration NaCl solutions is studied. Based on this studying, the coefficients of water recovery are improved and energy consumption per ton fresh water is reduced, which provides a reference for DCMD producing fresh water from seawater.

2. Theory

DCMD uses a porous, hydrophobic membrane with liquids in direct contact with both surfaces of the membrane. The driving force is a temperature-induced vapor pressure difference caused by having a hot feed and a cold permeate. Fig. 1 illustrates the heat transfer process. Heat is first transferred from the heated feed solution of uniform temperature T_f across the heat boundary layer to the membrane surface at a rate Q_f . At the surface of the membrane, liquid is vaporized, and heat is transferred across the membrane at a rate $N\Delta H$. Additionally, heat is conducted through the membrane material and the vapor that fills the pores at a rate $(k_m/\delta)(T_{fm} - T_{pm})$. Total heat transfer across the membrane includes conduction and evaporation. Conduction is treated as a heat loss mechanism as no corresponding mass transfer takes place. Finally, as vapor condenses at the

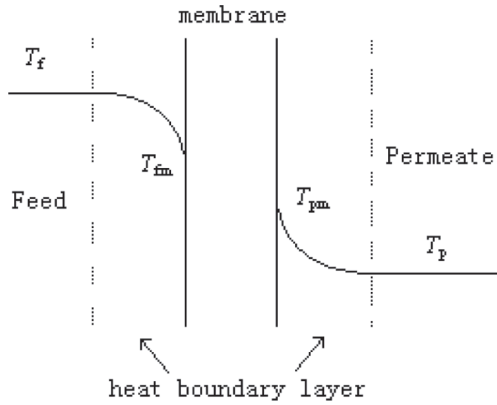


Fig. 1. The heat transfer process of DCMD.

liquid–vapor interface, heat is removed from the cold-side membrane surface through the heat boundary layer at a rate $h_p (T_{pm} - T_p)$. Boundary layers next to the membrane can contribute substantially to the overall heat transfer resistance. Heat transfer across the boundary layers is often the rate-limiting step for mass transfer in MD, because such a large quantity of heat must be supplied to surface of the membrane to vaporize the liquid.

$$Q_f = h_f (T_f - T_{fm}) \tag{1}$$

$$Q_m = N\Delta H + \frac{k_m}{\delta} (T_{fm} - T_{pm}) \tag{2}$$

$$Q_p = h_p (T_{pm} - T_p) \tag{3}$$

According to conservation of energy:

$$Q_f = Q_m = Q_p \tag{4}$$

The relations of ΔH and temperature and concentration of NaCl solution are studied, respectively. Concentration of NaCl solution hardly affects ΔH . The effect of temperature on ΔH must be considered.

$$\Delta H = \Delta H_{pm} + C_p (T - T_{pm}) \tag{5}$$

$$\Delta H_{pm} = 2258.4 + C_p (373.15 - T_{pm}) \tag{6}$$

where $C_p = 1900 \text{ J/kgK}$, by substitution of Eq. (6) into (5) and rearranging:

$$\Delta H = \Delta H^o + C_p (T - 2T_{pm}) \tag{7}$$

where $\Delta H^o = 2967.385 \text{ kJ/kg}$.

Eq. (2) can be converted to

$$Q_m = N\Delta H - k_m \frac{dT}{dx}$$

By combining Eqs (1), (3), (4) and (7) and rearranging, the temperatures of the layers adjacent to the membrane can be obtained as:

$$\left\{ \begin{aligned} T_{fm} &= \frac{\left[1 - \exp\left(-NC_p \frac{k_m}{\delta}\right) \right] (h_f T_f - N\Delta H^o) + NC_p \left(T_p + \frac{h_f}{h_p} T_f \right) \left[2 - \exp\left(-NC_p \frac{k_m}{\delta}\right) \right]}{h_f \left[1 - \exp\left(-NC_p \frac{k_m}{\delta}\right) \right] + NC_p \left\{ 1 + \frac{h_f}{h_p} \left[2 - \exp\left(-NC_p \frac{k_m}{\delta}\right) \right] \right\}} \\ T_{pm} &= \frac{\left[1 - \exp\left(-NC_p \frac{k_m}{\delta}\right) \right] (h_p T_p + N\Delta H^o) + NC_p \left(T_f + \frac{h_p}{h_f} T_p \right)}{h_p \left[1 - \exp\left(-NC_p \frac{k_m}{\delta}\right) \right] + NC_p \left[2 + \frac{h_p}{h_f} - \exp\left(-NC_p \frac{k_m}{\delta}\right) \right]} \end{aligned} \right. \tag{8}$$

Our DCMD experiments kept the same general pressure on both the feed and the permeate, so Poiseuille flow can be ignored. For 0~100°C, the mean free molecular path of the gaseous water molecules is about 0.2 μm as same as the pore diameter of experiments membrane, and vapor diffusion coefficient D_{WA} of molecular diffusion model and D_{KW} of Knudsen diffusion model are in the same order of magnitude, so in the apertures, collisions between molecule — molecule and molecule — aperture wall must be considered. That is to say, DCMD mass transfer process is an intergradation diffusion, which includes Knudsen diffusion and molecular diffusion. In most cases, the models suggest that the flux (N) may be written as a linear function of the transmembrane vapor pressure difference.

$$N = \frac{P_{fm} - P_{pm}}{R_m(t) + R_c(t) + R_f(t)} \quad (9)$$

and

$$\frac{1}{R_m(t)} = \frac{\tau \delta R T_{av}}{\epsilon M_w D_{KA}} + \frac{\tau \delta Y_{ln} R T_{av}}{\epsilon M_w P D_{WA}} \quad (10)$$

where $R_m(t)$ is the membrane resistance, $R_c(t)$ is the concentration polarization resistance, $R_f(t)$ is the membrane fouling resistance, Y_{ln} is the logarithm mean pressure of air. Knudsen diffusion coefficient D_{KW} and molecular diffusion coefficient D_{WA} are calculated by:

$$D_{KW} = 97r \left(\frac{T}{M_w} \right)^{0.5} \quad (11)$$

$$D_{WA} = \frac{0.00143T^{1.75} \left(\frac{1}{M_w} + \frac{1}{M_A} \right)^{0.5}}{P \left[(v_w)^{1/3} + (v_A)^{1/3} \right]^2} = 1.19 \times 10^{-4} \frac{T^{1.75}}{P} \quad (12)$$

where $v_w = 13.1 \text{ cm}^3/\text{mol}$, $v_A = 19.7 \text{ cm}^3/\text{mol}$, $P = 101.35 \text{ kPa}$.

For high concentration feed, when concentrations of the layers adjacent to the membrane are calculated, concentration polarization must be considered. In desalination, the solutes are retained by the membrane and accumulate on the membrane surface. Therefore, the feed membrane surface concentration will gradually increase. Such a concentration buildup will generate a diffusive flow back to the bulk of the feed. When steady-state conditions are established, the convective solute flow to the membrane surface will be balanced by the solute flux through the membrane plus the diffusive flow from the membrane surface back to the bulk (Fig. 2). When solute rejection is assumed as 100%, mathematically, this phenomenon can be described as

$$\frac{c_{fm}}{c_f} = \exp\left(\frac{N}{k_c \rho}\right) \quad (13)$$

Eq. (13) shows that the concentration polarization is related to flux, mass transfer coefficient, feed density and feed concentration. When vapor transfer across membrane is the rate-limiting step for mass transfer in MD, flux mainly depends on membrane resistance. When mass transfer across the boundary layers is the rate-limiting step for

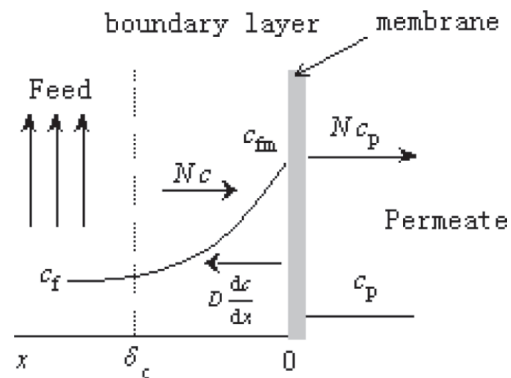


Fig. 2. Feed concentration distribution.

mass transfer in MD, flux mainly relies on the concentration polarization resistance. Mass transfer coefficient can be affected by many factors, which include flow rate, viscosity and density of feed, solute diffusion coefficient, convective solute transfer coefficient and characteristic length. However viscosity and density of feed, solute diffusion coefficient and convective solute transfer coefficient are directly related to the concentration and temperature of feed. So main factors that affect mass transfer coefficient are concentration, temperature and flow rate. That is to say, $R_c(t) = f(v, c_f, T)$. Because decrease of feed concentration, increase of flow rate and feed temperature can enhance flux and reduce concentration polarization resistance, concentration polarization resistance is expressed as follows

$$R_c(t) = A \frac{c_f^x}{v^z T^y} \quad (14)$$

where x , y and z are determined by experiments and A is a constant. The mass transfer correlation can be written by [8].

(1) For laminar flow: Graetz–Leveque equation

$$\text{Sh} = 1.86 \left(\text{Re} \text{Sc} \frac{d_h}{L} \right)^{1/3} \quad (15)$$

(2) For turbulent flow: Dittus–Boelter equation.

$$\text{Sh} = 0.023 \text{Re}^{0.8} \text{Sc}^{0.33} \quad (16)$$

The spacer was filled in the flow channel, so V is calculated by

$$V = \frac{Q}{A \epsilon_s} \quad (17)$$

$$d_h = \frac{4 \epsilon_s}{2/h_{sp} + (1 - \epsilon_s) S_{vsp}} \quad (18)$$

$$S_{vsp} = 4/d_f \quad (19)$$

$$\epsilon_s = 1 - \frac{\pi d_f^2}{2l_m h_{sp} \sin \theta} \quad (20)$$

Vapor pressure of pure water is given by Antoine's equation

$$P^o = \exp \left(23.238 - \frac{3841}{T - 45} \right) \quad (21)$$

Vapor pressure of feed is given by

$$P = P^o (1 - x) (1 - 0.5x - 10x^2) \quad (22)$$

Heat transfer coefficients can be calculated by heat transfer correlation. Substituting heat transfer coefficients into (8) leads to temperatures in the layers adjacent to the membrane, with which vapor pressure can be obtained in Eq. (22). Finally, flux can be given by using Eq. (9).

3. Experimental

These experiments were carried out in the School of Chemical Engineering and Industrial Chemistry at the University New South Wales. The flow chart is shown in Fig. 3. The instruments involved in the experiments were: constant temperature heater, MUSTERFLEX double-barreled creeping motion pump, 1-7013/DA/D transducer, Melder-Toledo electric balance and refrigeration.

The membrane module which was the key of DCMD was made from Perspex (polymerized methylmethacrylate) with a flow channel 40 mm wide, 100 mm long, and 2.5 mm high. The effective membrane area was 0.004 m². In all experiments the membrane module was placed in the horizontal position. Pure water was used as the cold liquid. Pure water and high concentration NaCl solution was used as the feed, respectively.

Table 1
Information of the membranes and spacers employed in experiments

Membrane	Name	Material	Producer	Pore size, μm	Heat conduction coefficient, $\text{W}\cdot\text{m}^{-1}\cdot\text{K}^{-1}$	Thickness, μm	Porosity
	GVSP	PVDF	Millipore	0.22	0.14	120	0.75
	GVHP	PVDF	Millipore	0.20	0.14	125	0.80
Spacer	$h_{sp}\times 10^3, \text{m}$	$d_f\times 10^3, \text{m}$	$l_m\times 10^3, \text{m}$	Porosity, ϵ_s	S_{vsp}, m^{-1}	$d_s\times 10^3, \text{m}$	Angle, θ
	1.15	0.55	2.8	0.852	7273	1.21	90

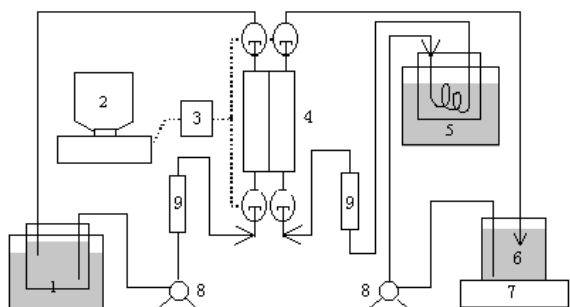


Fig. 3. Experimental flow chart (1 hot water bath, 2 computer, 3 A/D transducer, 4 flowmeter, 5 pump, 6 electric balance, 7 tank for permeate, 8 cold water bath, 9 flow meter).

The membrane structure parameters are listed in Table 1.

The feed solution was heated and maintained at the required temperatures in a constant temperature heater. The pump produced the same flow rates for both the feed and the permeate flows. After a long period of running, membrane maybe was fouled, which would affect the flux and rejection. Therefore, the membrane was used under 10 h for experiments, the membrane fouling resistance $R_f(t)$ could be ignored.

The parameters of Eq. (16), A , x , y and z , are determined by experiments. We changed one factor and fixed other factors for DCMD experiments with PVDF membranes. Then the relations of concentration polarization resistance and concentrations of NaCl solutions, flow rates and feed

temperatures were regressed numerically. For our experiments, $A = 4.05 \times 10^{11}$, $x = 3.5$, $y = 1.45$, $z = 0.56$.

4. Results and discussion

DCMD mechanism for pure water and dilute solution has been intensively studied by many researchers [3,8]. In this paper, we focused on study of DCMD mechanism for high concentration NaCl solution. To contrast with that, the model was first tested in pure water experiments. In Figs. 4 and 5, fluxes are shown with respect to the bulk temperature for pure water at the same operational condition for GVHP and GVSP membranes, respectively. In these cases, concentration polarization resistance and membrane-fouling resistance could be ignored for a short runtime. The model-predicted mass flux is close to the measured mass fluxes. The differences between the calculated and measured mass fluxes vary less than 5%.

The flux increases slightly when the recirculation rate increases for NaCl solution (Figs. 6, 7). The intention of using the higher re-circulation rate was to increase the heat transfer coefficient and thus reduce the effect of temperature polarization and concentration polarization. This means that the temperatures at the membrane surface approximate more closely that of the bulk streams, and thus the transmembrane temperature difference is larger. This produces a larger driving force and consequently enhances the flux. The

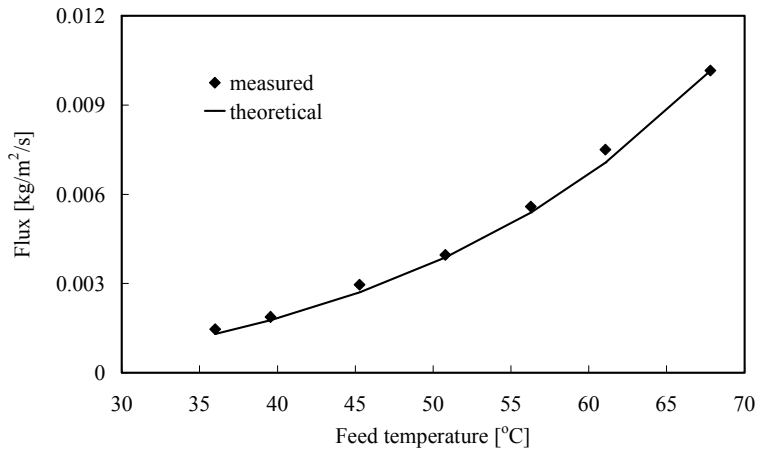


Fig. 4. Flux vs. feed temperature for pure water experiment, GVSP, flow rate: 0.145 m/s, T_p : 19.7°C.

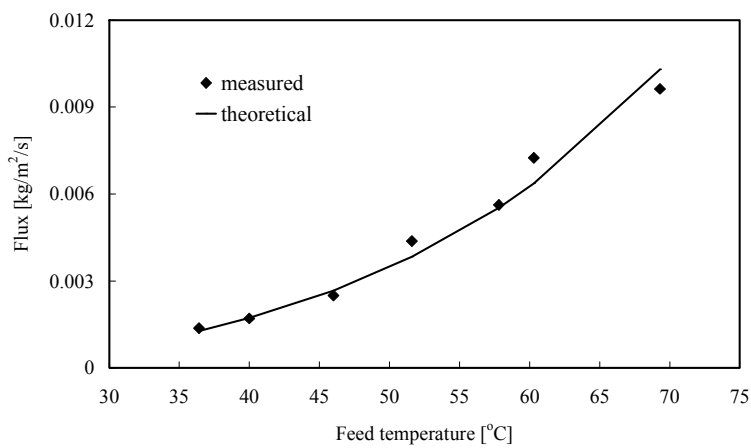


Fig. 5. Flux vs. feed temperature for pure water experiment, GVHP, flow rate: 0.145 m/s, T_p : 19.7°C.

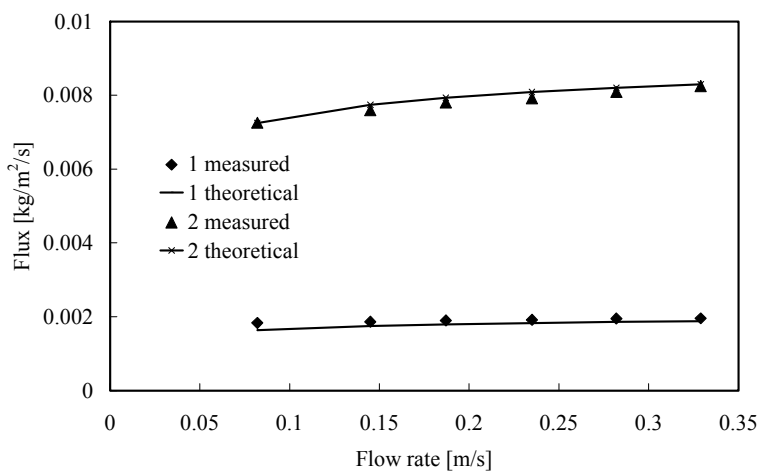


Fig. 6. Effect of flow rate on flux, GVHP, concentration of NaCl: 17.76%, flow rate: 0.145 m/s, T_p : 20.5°C, T_{f1} : 43.2°C, T_{f2} : 68°C.

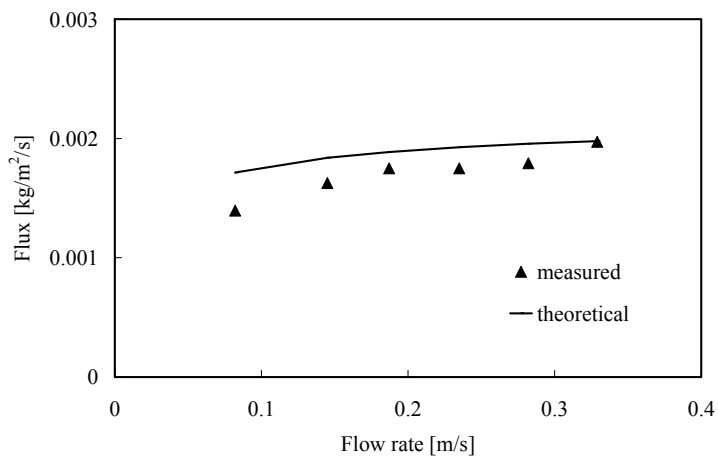


Fig. 7. Effect of flow rate on flux, GVSP, concentration of NaCl: 24.68%, flow rate: 0.145 m/s, T_p : 20.5°C, T_f : 43.2°C.

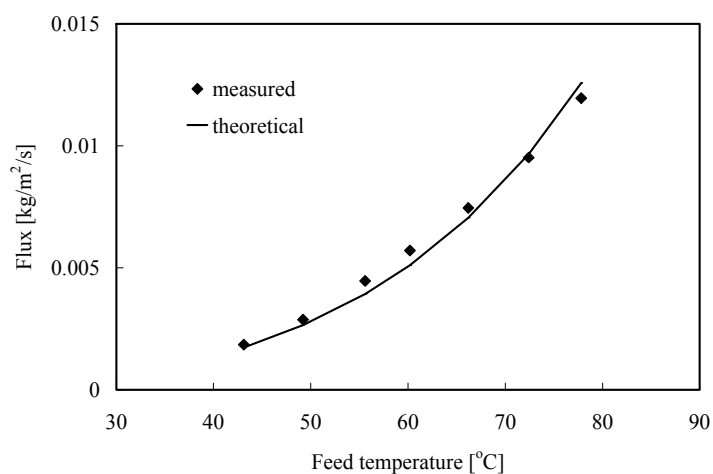


Fig. 8. Effect of feed temperature on flux, GVHP, concentration of NaCl: 17.76%, flow rate: 0.145 m/s, T_p : 20.5°C.

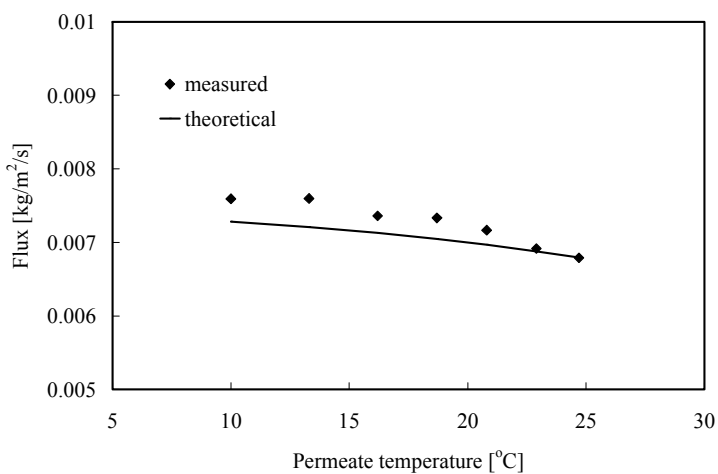


Fig. 9. Effect of permeate temperature on flux, GVHP, concentration of NaCl: 17.76%, flow rate: 0.145 m/s, T_p : 66°C.

effect of feed flow rate on water flux is less than that of the feed temperature.

Fig. 8 shows the relationship between the flux and the feed bulk temperature for NaCl solution. In this experiment, flow rates, concentrations of NaCl solution and the permeate temperatures were 0.145 m/s, 17.76% and 20.5°C, respectively. These experiments were conducted with a GVHP membrane and a shorter runtime. An increase in flux was observed when the feed temperature was raised from 40°C to 80°C. This can be attributed to several factors: increase of vapor pressure due

to the feed temperature, reduction of concentration polarization resistance and increase of temperature polarization. The results from this figure show the relation of the concentration polarization resistance and the feed temperature. Similarly, Fig. 9 shows water fluxes measured at different the permeate temperatures, when flow rates, concentrations of NaCl solution and the permeate temperatures were 0.145 m/s, 17.76% and 66°C, respectively. The water flux increased slightly as the permeate temperatures decreased. For GVSP membrane, the same rule applies (see Figs. 10, 11).

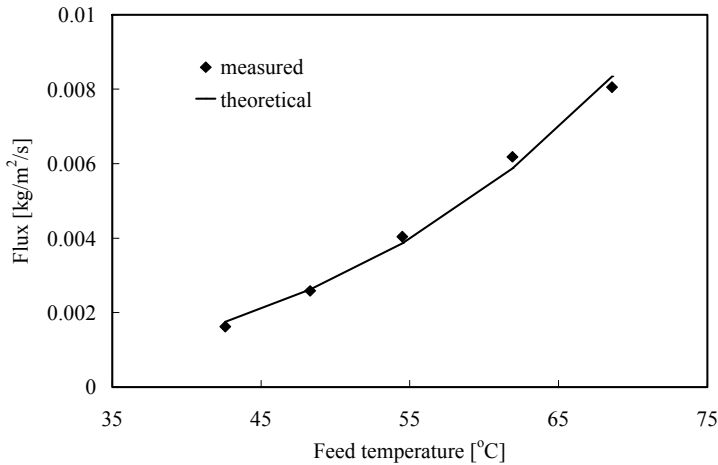


Fig. 10. Effect of feed temperature on flux, GVSP, concentration of NaCl: 24.68%, flow rate: 0.145 m/s, T_p : 20.5°C.

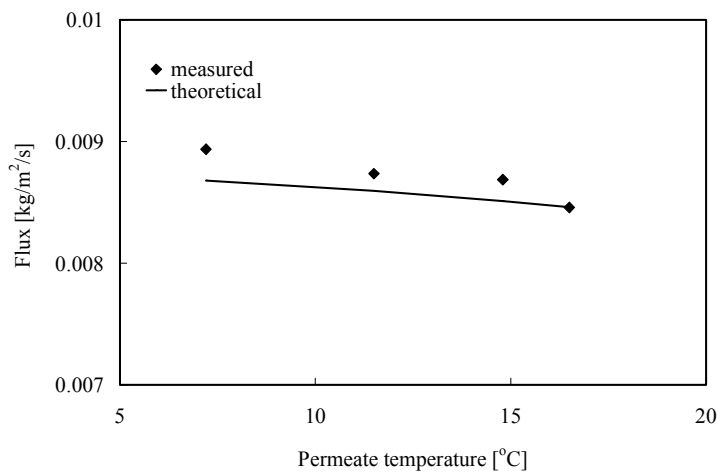


Fig. 11. Effect of permeate temperature on flux, GVSP, concentration of NaCl: 24.68%, flow rate: 0.145 m/s, T_p : 68.6°C.

For high concentration NaCl solution, water fluxes vary with the feed concentration according to inverse “S” shape (see Figs. 12, 13), this is the most important difference between high concentration NaCl solution and dilute NaCl solution. It is clearly seen that the variation of flux with time can be divided into three states: sub-steady, pre-steady and steady states. In the sub-steady state, the flux drops slightly with time. After reaching pre-steady state, the flux begins to decline significantly for 30 min until it reaches the steady state. For different operation conditions, the steady state fluxes are different, such as

1.33×10^{-3} kg/m²/s for Fig. 12, 5.8×10^{-4} kg/m²/s for Fig. 13. And we found that the concentration of the starting point of pre-steady state was about 26% for our experiments. When the NaCl solution is saturated, the water flux reaches the steady state. However, in the high concentration NaCl solution DCMD experiments, it is difficult to predict the water flux by using any existing models, such as Knudsen diffusion model, molecular diffusion model and Poiseuille flow model. The differences between the calculated and measured mass fluxes varied less than 10% for sub-steady state; while for pre-steady state and steady state, the dif-

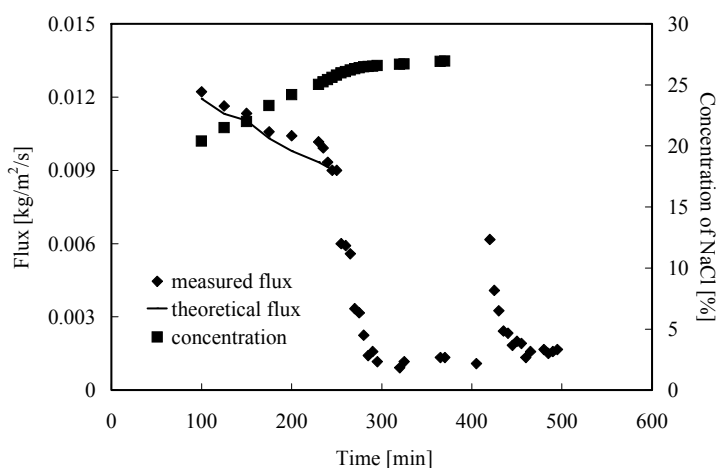


Fig. 12. The result of bath operation, GVHP, concentration of NaCl: 17.76%, flow rate: 0.145 m/s, T_f : 79°C, T_p : 20.5°C.

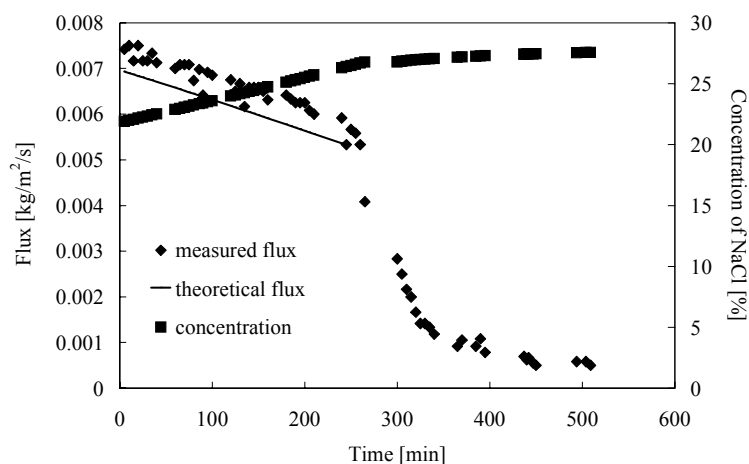


Fig. 13. The result of bath operation GVSP, concentration of NaCl: 24.68%, flow rate: 0.145 m/s, T_f : 68.5°C, T_p : 20.6°C.

ferences are rather large. The reasons are as follows.

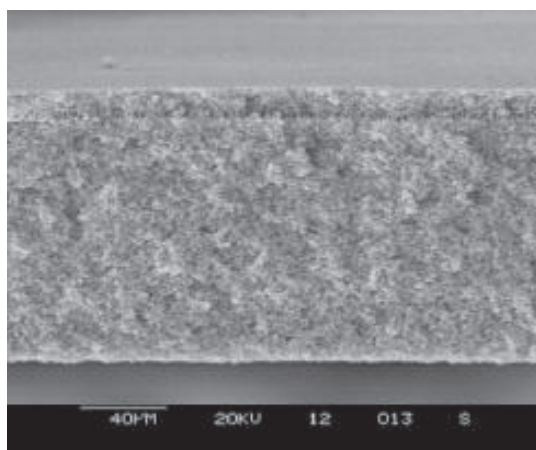
When the concentration of NaCl solution is far from saturation, the mass transfer coefficient is calculated with bulk solution data. While concentration of NaCl solution is about 26%, the membrane surface concentration has reached saturation. Therefore the solution of the boundary layer differs greatly from the bulk solution such that the concentration polarization resistance and membrane fouling resistance increase sharply. In the experiments, we could find any crystal on the membrane surface (Fig. 14). For analyzing membrane fouling resistance (Fig. 12), stir firstly was stopped when runtime was 405 min. Immediately a large amount of crystals formed on the interface of the feed and air on the hot tank wall while fluxes went up simultaneously. When runtime was 480 min, 500 ml pure water was injected into the hot tank. But no flux change was observed. Taking out the membrane, we found that the membrane had been fouled severely. This indicates that membrane-fouling resistance is the major factor at steady state.

5. Conclusions

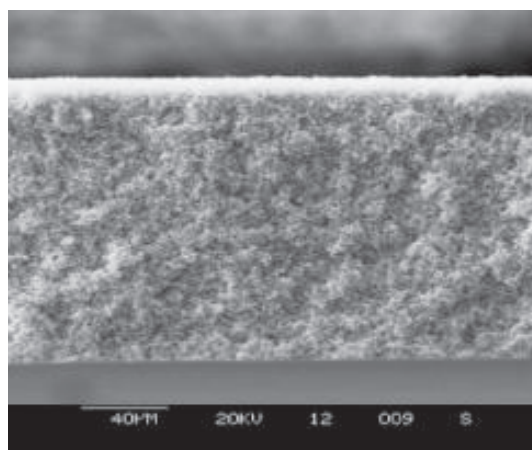
A model was set up by DCMD experiments for high concentration NaCl solution. The difference of the calculated and measured mass flux was less than 10%. For high concentration NaCl solution, Water fluxes were observed to increase with increase of feed temperature and flow rate and decrease of permeate temperature and concentration of NaCl solution. When concentration of NaCl solution was close to saturation, water fluxes began to decrease sharply. After the concentration of NaCl solution was saturated, water fluxes approached a steady state gradually. Variation of membrane-fouling resistance accounts for the observation above. So for high concentration salt solution DCMD experiments, membrane fouling must be regarded highly.

Acknowledgements

The authors would like to thank Australia–China Institutional Links Program for financial support and thank the UNESCO Center for Membrane Science and Technology for hospitality.



(a) brand-new membrane



(b) used membrane

Fig. 14. SEM of new membrane and used membrane.

Symbols

d_h	— Hydraulic radius, m
h	— Convective heat transfer coefficient, $W \cdot m^{-2} \cdot K^{-1}$
ΔH	— Latent heat of water, $J \cdot kg^{-1}$
k	— Heat conduction coefficient, $W \cdot m^{-1} \cdot K^{-1}$
k_c	— Mass transfer coefficient, $m \cdot s^{-1}$
M	— Molecular weight, $g \cdot mol^{-1}$
N	— Mass flux across membrane, $kg \cdot m^{-2} \cdot s^{-1}$
Nu	— Nusselt number
p^o	— Vapor pressure, Pa
Pr	— Prandtl number
Q	— Heat flux, $W \cdot m^{-2}$
r	— Radius of the membrane pore size, m
Re	— Reynolds number
Sc	— Schmidt number
Sh	— Sherwood number
T	— Temperature, K

Greek

δ	— Membrane thickness, m
ε	— Porosity
μ	— Viscosity, Pa·s
ρ	— Solution density, $kg \cdot m^{-3}$
τ	— Membrane tortuosity

Subscripts

f	— The bulk of the feed
fm	— Membrane surface of the feed
p	— The bulk of the permeate

pm	— Membrane surface of the permeate
m	— Membrane
W	— Water
A	— Air
av	— Average

References

- [1] K.W. Lawson and D.R. Lloyd, Membrane distillation. *J Membr. Sci.*, 124 (1997) 1–25.
- [2] A. Burgoyne and M.M. Vahdati, Direct contact membrane distillation. *Separ. Sci. Technol.*, 35 (2000) 1257–1284.
- [3] R.W. Schofield, A.G. Fane and C.J.D. Fell, Heat and mass transfer in membrane distillation, *J Membr. Sci.*, 33 (1987) 299–313.
- [4] M. Gryta, M. Tomaszewska, J. Grzechulska and A.W. Morawski, Membrane distillation of NaCl solution containing natural organic matter. *J. Membr. Sci.*, 181 (2001) 279–287.
- [5] F. Lagana, G. Barbieri and E. Drioli, Direct contact membrane distillation: modelling and concentration experiments. *J. Membr. Sci.*, 166 (2000) 1–11.
- [6] S. Kimura and S.-I. Nakao, Transport phenomena in membrane distillation. *J. Membr. Sci.*, 33 (1987) 285–298.
- [7] F.A. Banat and J. Simandl, Desalination by membrane distillation: A parametric study. *Separ. Sci. Technol.*, 33 (1998) 201–226.
- [8] L. Martinez-Diez, F.J. Florido-Diaz and M.I. Vazquez-Gonzalez, Study of polarization phenomena in membrane distillation of aqueous salt solutions. *Separ. Sci. Technol.*, 35 (2000) 1485–1501.